Determination of γ and Stereospecific Assignment of H5′ Protons by Measurement of ^2J and ^3J Coupling Constants in Uniformly ^{13}C Labeled RNA

J. P. Marino, H. Schwalbe, S. J. Glaser, and C. Griesinger*

Contribution from the Institut für Organische Chemie, Universität Frankfurt, Marie-Curie Strasse 11, Frankfurt/Main, Germany D-60439

Received October 24, 1995[⊗]

Abstract: The conformational analysis of the backbone angle γ (O5′−C5′−C4′−C3′) and the stereospecific assignment of the H5′$^{(pro\text{-}S)}$, H5′$^{(pro\text{-}R)}$ diastereotopic protons in a uniformly ^{13}C,^{15}N labeled RNA oligonucleotide was performed using new Exclusive COSY (E.COSY) type multidimensional heteronuclear NMR experiments designed to measure ^3J(H4′,H5′) homonuclear and ^2J(C4′,H5′) heteronuclear coupling constants. The experiments were demonstrated on a uniformly ^{13}C,^{15}N labeled 19-mer RNA hairpin (5′-rGCACCGUUGGUAGCGGUGC-3′) derived from the RNA I transcript involved in *Col E1* replication control. From the small ^3J(H4′,H5′) couplings constants observed for the RNA hairpin, it was concluded that all γ angles assume a gauche$^+$ rotamer conformation ($\gamma = 60°$). From the signs of the ^2J(C4′,H5′) coupling constants, the H5′ protons were stereospecifically assigned. In the helical stem region of the hairpin, the H5′$^{(pro\text{-}S)}$ protons were found to resonate downfield (∼0.4 ppm) of the H5′$^{(pro\text{-}R)}$ protons. In the loop region of the hairpin, the chemical shift differences between the H5′$^{(pro\text{-}S)}$, H5′$^{(pro\text{-}R)}$ resonances were found to be smaller, and in most cases, the H5′$^{(pro\text{-}S)}$ protons were found to resonate upfield of the H5′$^{(pro\text{-}R)}$ protons. The different chemical shift patterns observed for the H5′$^{(pro\text{-}S)}$ and H5′$^{(pro\text{-}R)}$ protons in the two secondary structure elements are discussed.

Introduction

The quality of structures determined by NMR spectroscopy relies on the extent to which a full interpretation can be made of the experimentally determined NOEs and *J* coupling constants. To this end, the unambiguous assignment of NOE distances and torsion angles to one of two diastereotopic groups can provide a significant improvement in the use of NOE distance and torsion angle constraints in NMR structure determination.[1−4] In RNA and DNA oligonucleotides, assignment of NOE distances, and *J* coupling constants stereospecifically to one of the two H5′ protons is rather critical for the precise determination of nucleic acid backbone geometry.[3,4] The NOEs and coupling constants that involve the H5′ diastereotopic protons not only define the backbone torsion angle γ (O5′−C5′−C4′−C3′) but also can reveal other long-range correlations either within the given ribose or along the oligonucleotide backbone. In particular, stereospecific assignment of the H5′ protons can be critical for determining the angle β (P5′−O5′−C5′−C4′) by allowing the stereospecific assignment of the heteronuclear ^3J(H5′,P) coupling constants.

Previous methods for stereospecific assignment of H5′ protons in oligonucleotides have included the use of the proton chemical shifts,[5] the interpretation of NOEs together with small homonuclear ^3J(H,H) couplings[6,7] and stereoselective deuteration.[8] In DNA, empirical rules based on chemical shift arguments have been used quite successfully to stereospecifically assign the H2′ diastereotopic protons. In most cases, the H2′$^{(pro\text{-}S)}$ proton is found to resonate upfield of the H2′$^{(pro\text{-}R)}$ proton.[7] A similar chemical shift analysis has been proposed for the stereoselective assignment of H5′ protons found in the context of a canonical A-form RNA conformation,[5] according to which the H5′$^{(pro\text{-}S)}$ proton resonates downfield from H5′$^{(pro\text{-}R)}$. In sum, however, the chemical shift approach to stereospecific assignment has obvious fallibilities such as inapplicability in regions of noncanonical structure or in the presence of bound ligands.

The use of measured or estimated ^3J(H4′,H5′) couplings about γ combined with a comparison of the relative intensities of the H3′, H5′$^{(pro\text{-}S)}$ and H3′, H5′$^{(pro\text{-}R)}$ cross peaks in a 2D NOESY (nuclear Overhauser effect spectroscopy) experiment[3,6] has also been used for stereospecific assignment in oligonucleotides (e.g., if $\gamma = 60°$ as determined from small ^3J(H4′,H5′) couplings, the distances d(H3′,H5′$^{(pro\text{-}R)}$) and d(H3′,H5′$^{(pro\text{-}S)}$) should differ by ∼1.5 Å). Although this method has been applied with some success to small DNA oligonucleotides, it has been quite limited in application to RNA oligonucleotides due to the extremely poor resolution of the ribose (H2′, H3′, H4′, and H5′) protons. NOE-based methods for stereospecific assignment may also be subject to errors due to spin diffusion or conformational averaging.

In comparison to methods based on the interpretation of chemical shifts and NOEs, the synthesis of stereospecifically deuterated samples is a much more precise and unambiguous method for stereospecific assignment.[8] It, however, has the drawback of requiring the stereoselective synthesis of additional samples for the sole purpose of stereospecific assignment. It is therefore of great interest to establish an alternative robust experimental method for determining the stereospecific assignments of H5′ diastereotopic protons in oligonucleotides.

* To whom correspondence should be addressed.

⊗ Abstract published in *Advance ACS Abstracts,* April 1, 1996.

(1) Sherman, S. A.; Johnson, M. E. In *Proteins*; Renugoplakrishnan and Venkatesan, Eds.; ESCOM: Leiden, The Netherlands, 1991; pp 62−67.

(2) Wüthrich, K. In *Proteins*; Regugoplakrishnan and Venkatesan, Eds.; ESCOM: Leiden, The Netherlands, 1991; pp 3−10.

(3) Varani, G.; Tinoco, I., Jr. *Q. Rev. Biophys.* **1991**, *24*, 479−532.

(4) van de Ven, F. N.; Hilbers, C. W. *Eur. J. Biochem* **1988**, *178*, 1−38.

(5) Remin, M.; Shugar, D. *Biochem. Biophys. Res. Commun.* **1972**, *48*, 636−642.

(6) Blommers, M. J. J.; van de Ven, F. J. M.; van der Marel, G. A.; van Boom, J. H.; Hilbers, C. W. *Eur. J. Biochem.* **1991**, *201*, 33−51.

(7) Wijmenga, S. S.; Mooren, M. M. W.; Hilbers, C. W. In *NMR of Macromolecules, A Practical Approach*; Roberts, G. C. K., Ed.; Oxford University Press: Oxford, U.K., 1993.

(8) Kline, P. C.; Serianni, A. S. *Magn. Reson. Chem.* **1988**, *26*, 131−138. Tate, S.; Kubo, Y.; Ono, A.; Kainosho, M. *J. Am. Chem. Soc.* **1995**, *117*, 7277−7278.

S0002-7863(95)03554-2 CCC: $12.00 © 1996 American Chemical Society

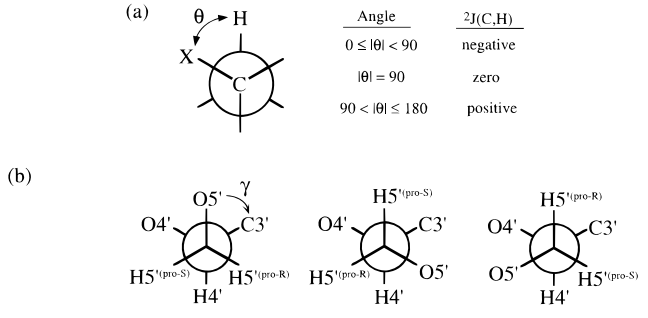

rotamer	I	II	III
γ angle	60° (gauche+)	- 60° (gauche-)	180° (trans)
^3J(H4′,H5′(pro-S))	small	large	small
^3J(H4′,H5′(pro-R))	small	small	large
^2J(C4′,H5′(pro-S))	negative	negative	positive
^2J(C4′,H5′(pro-R))	positive	negative	negative

Figure 1. (a) Newman projection showing the sign dependence of the ^2J(C,H) on the angle θ for a generalized XC−CH fragment. (b) Newman projection around γ with the predicted signs and coupling constants for the three rotamer states (gauche$^+$, trans, and gauche$^-$).

From work on model systems it has been established that in an H−C−C−X system, where X is an electronegative atom, the sign of the ^2J(C,H) coupling shows a dependence (Figure 1a) on the torsion angle θ between H and X.[9] From theoretical calculation on ethanol, the ^2J(C,H) was found to be negative when $0° < |\theta| \leq 90°$, zero when $|\theta| = 90°$, and positive when $90° < |\theta| \leq 180°$, with maximum values observed for 0° and 180°. Hines and co-workers[10] exploited this ^2J correlation and showed that the sign dependence (Figure 1b) of the ^2J(C4′, H5′) coupling constants associated with γ could be used both to stereospecifically assign the H5′ protons and to determine the conformation of the γ angle. Using a 30% ^{13}C labeled UUCG tetraloop RNA sample, stereospecific assignments for the H5′ protons were obtained from the sign of the ^2J(C4′,H5′) coupling constants measured using E.COSY patterns observed in X-filtered NOESY and TOCSY (total correlation spectroscopy) experiments.[11] The X-filtered experiments used in these studies, however, suffered from insensitivity and cross peak overlap to such an extent that only the ^2J(C4′,H5′) coupling constants for three out of 12 residues were reported.

In this paper, we report new sensitive heteronuclear NMR methods that measure the homonuclear ^3J(H4′, H5′) and heteronuclear ^2J(C4′,H5′) coupling constants in uniformly ^{13}C labeled oligonucleotides.[12−15] A "directed" HCC-TOCSY-CCH-E.COSY tailored for the measurement of vicinal ^3J(H4′,H5′) coupling constants and a family of C5′,H5′-selective experiments for the measurement of geminal ^2J(C4′,H5′) coupling constants are presented. The coupling constants measured using these NMR experiments have provided fairly complete stereospecific assignment of H5′ protons and allowed analysis of the conformation about all the γ backbone angles in the 19-mer RNA hairpin under investigation.

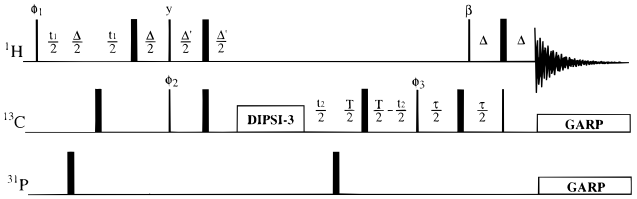

Figure 2. Pulse sequence for the "directed" HCC-TOCSY-CCH-E.COSY used for the determination of ^3J(H4′,H5′) coupling constants in this study. The details of the parameters used to implement this pulse sequences are given in part B of the Experimental Section.

NMR Experiments

A. Measurement of ^3J(H4′,H5′) Coupling Constants. In order to increase resolution, ^3J(H4′,H5′) homonuclear coupling constants were measured using a "directed" HCC-TOCSY-CCH-E.COSY experiment[16,17] as shown in Figure 2. The "directed" HCC-TOCSY-CCH-E.COSY experiment first excites proton magnetization, which is frequency labeled in t_1 and then transferred via a refocused INEPT step into in-phase carbon magnetization. The refocusing period ($\Delta' = 3.0$ ms), duration of the isotropic C,C-TOCSY mixing period (DIPSI-3 during $\tau_1 = 13.5$ ms), and ^{13}C constant time evolution delay ($T = 7.6$ ms) that are then applied have been exactly matched such that coherence originating from H1′ during t_1 frequency labeling forms predominantly "forward directed" antiphase coherence of the type $2S_{i,y}S_{i+1,z}$ (with $i = 3, 4$; 1 = C1′, 2 = C2′, 3 = C3′, 4 = C4′ and 5 = C5′) at the end of the constant time evolution.[17] Finally, a ^{13}C COSY (correlation spectroscopy) pulse is applied and a reversed DEPT is utilized for the C → H back-transfer step[18] with a small flip angle proton pulse ($\beta = 45°$)[19,20] applied to meet the E.COSY requirement of leaving the spin state of the passive spins (the H3′ and H4′ protons in this experiment) unperturbed. In this experiment, the undesired coherence transfer between nonconnected transitions that results from the β pulse is removed by a post-acquisition processing procedure.[22] The experiment allows both the correlation of the HCCH-E.COSY[21,22] cross peaks (Figure 5a) with the usually well resolved H1′ chemical shifts within a given ribose and the extremely selective coherence transfer within the ribose spin system. As a result, the experiment yields well-resolved C4′, H5′ cross peaks that are normally overlapped in the standard 2D HCCH-E.COSY[22] with the autocorrelated C4′, H4′ cross peaks and the backward-directed C4′, H3′ cross peaks.

The "directed" TOCSY principle relies on a judicious combination of isotropic and longitudinal mixing periods[23] in linear spin systems with uniform coupling constants. For an initial density operator $\sigma(0) = S_{1,x}$, isotropic mixing alone yields opposite signs but equal magnitudes of the expectation values of forward-directed coherence of spins i (i.e., $2S_{i,y}S_{i+1,z}$) and of

(9) Bock, K.; Pedersen, C. *Acta Chem. Scand.* **1977**, *B31*, 354−358. Cyr, N.; Perlin, A. S. *Can. J. Chem.* **1979**, *57*, 2504−2511. Schwarcz, J. A.; Cyr, N.; Perlin, A. S. *Can. J. Chem.* **1975**, *53*, 1872−1875.

(10) Hines, J. V.; Laundry, S. M.; Varani, G.; Tinoco, I., Jr. *J. Am. Chem. Soc.* **1993**, *115*, 11002−11003. Hines, J. V.; Landry, S. M.; Varani, G.; Tinoco Jr., I. *J. Am. Chem. Soc.* **1994**, *116*, 5823−5831.

(11) Edison, A. S.; Westler, W. M.; Markley, J. L. *J. Magn. Reson.* **1991**, *92*, 434−438. Wider, G.; Neri, D.; Otting, G.; Wüthrich, K. *J. Magn. Reson.* **1989**, *1991*, 426−431.

(12) Batey, R. T.; Inada, M.; Kujawinski, E.; Puglisi, J. D.; Williamson, J. R. *Nucleic Acids Res.* **1992**, 4515−4523. Nikonowicz, E. P.; Sirr, A.; Legault, P.; Jucker, F. M.; Baer, L. M.; Pardi, A. *Nucleic Acids Res.* **1992**, *20*, 4507−4513.

(13) Ono, A.; Tate, S.; Ishido, Y.; Kainosho, M. *J. Biomol. NMR* **1994**, *4*, 581−586.

(14) Quant, S.; Wechselberger, M. A.; Wolter, M. A.; Wörner, K.-H.; Schell, P.; Engels, J. W.; Griesinger, C.; Schwalbe, H. *Tetrahedron Lett.* **1994**, *35*, 6649−6652.

(15) Zimmer, D.; Crothers, D. M. *Proc. Natl. Acad. Sci. U.S.A.* **1995**, *92*, 3091−3095.

(16) Schwalbe, H.; Marino, J. P.; Glaser, S. J.; Griesinger, C. *J. Am. Chem. Soc.* **1995**, *117*, 7251−7252.

(17) Glaser, S. J.; Schwalbe, H.; Marino, J. P.; Griesinger, C. *J. Magn. Reson. B* **1996**, in press.

(18) Olsen, H. B.; Ludvigsen, S.; Sørensen, O. W. *J. Magn. Reson. A* **1993**, *104*, 226−230.

(19) Müller, L. *J. Magn. Reson.* **1987**, *97*, 191−194.

(20) Griesinger, C.; Sørensen, O. W.; Ernst, R. R. *J. Chem. Phys.* **1986**, *85*, 6837−6852.

(21) Griesinger, C.; Eggenberger, U. *J. Magn. Reson.* **1992**, *75*, 426−434.

(22) Schwalbe, H.; Marino, J. P.; Wechselberger, R.; Bermel, W.; Griesinger, C. *J. Biomol. NMR* **1994**, *4*, 631−644.

(23) Glaser, S. J. *J. Magn. Reson. A* **1993**, *104*, 283−301.

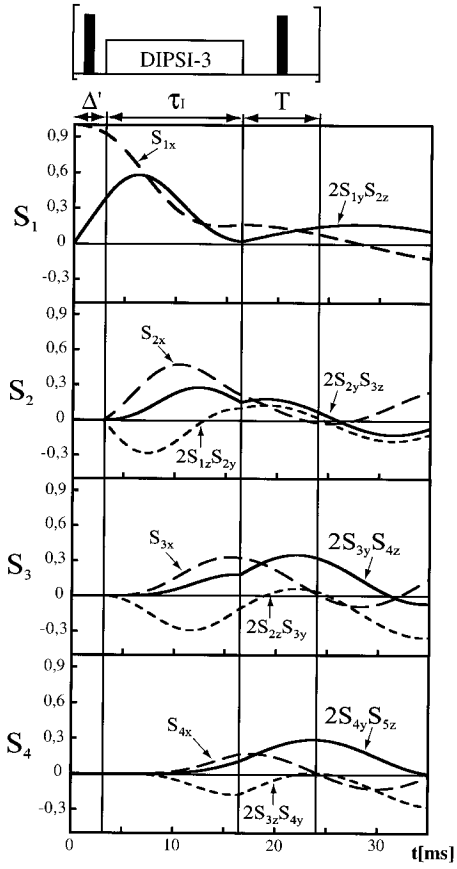

Figure 3. Plots of the evolution of the coherences of interest as a function of the constant time delay, T, for the spins $S_1 = C1'$ through $S_4 = C4'$ in a linear spin system ($S_1-S_2-S_3-S_4-S_5$) with approximately uniform coupling constants $^1J(C,C) = 40$ Hz and fixed delays of $\Delta' = 3.0$ ms and $\tau_I = 13.5$ ms. In each panel, the forward-directed coherences ($2S_{i,y}\,S_{i+1,z}$) are drawn as solid lines, while the backward directed ($2S_{i-1,z}S_{i,y}$) and in-phase coherence ($S_{i,x}$) are drawn as short and long dashed lines, respectively. Vertical lines through the four panels denote the durations of the three mixing periods Δ', τ_I, and T. At $T = 7.6$ ms, the forward-directed coherences $2S_{3y}S_{4z}$ and $2S_{4y}S_{5z}$ are close to their optimal values, while all other backward-directed and in-phase coherences are all close to zero.

backward-directed coherences of spin $i + 1$ (i.e., $2S_{i,z}S_{i+1,y}$) for all mixing times τ_I because of the conservation of coherence order. Hence, it is impossible to select forward-directed coherences ($2S_{i,y}S_{i+1,z}$) and suppress backward-directed coherences ($2S_{i,z}S_{i+1,y}$) and in-phase coherence ($S_{i,x}$) for all spins i using pure isotropic mixing experiments. However, this coherence transfer symmetry can be broken by additional periods of longitudinal mixing.[16,17] The optimal combinations of Δ', τ_I, and T delays needed to selectively generate forward-directed coherence transfer were found using a series of computer simulations in which weak $^{13}C-^{13}C$ coupling (longitudinal mixing) was assumed during the Δ' and T periods and ideal isotropic mixing conditions were assumed during the τ_I period. While the duration of $\Delta' = [2^1J(I,S)]^{-1} = 3.0$ ms was dictated by the heteronuclear coupling constant $^1J(C,H) = 160$ Hz, the duration of the isotropic mixing period could be varied to achieve the desired distribution of coherences along the linear spin system formed by $S_1 = C1'$ to $S_5 = C5'$ with approximately uniform coupling constants $^1J(C,C) = 40$ Hz. For the desired case in this paper, the optimum coherence transfer from S_1 to S_3 and S_4 was found using $\tau_I = 13.5$ ms. Figure 3 shows the evolution of the coherences of interest for fixed delays $\Delta' = 3.0$ ms and $\tau_I = 13.5$ ms and variable delays of T ($0 \le T \le 20$ ms). This simulation yields an optimal duration of the constant time evolution period of $T = 7.6$ ms, where the expectation values of almost all undesired in-phase and backward-directed coherences approach zero while the expectation values of the desired forward-directed coherences $2S_{3,y}S_{4,z}$ and $2S_{4,y}S_{5,z}$ are close to their optimal values.

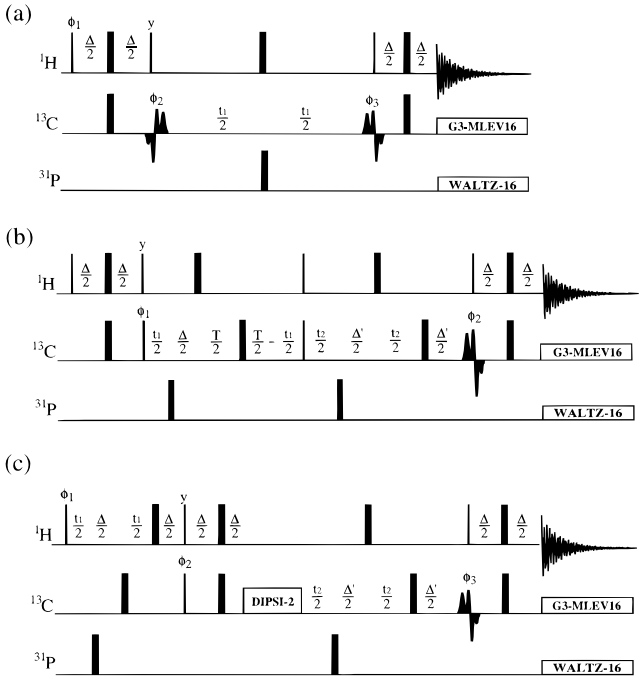

Figure 4. Pulse sequences for the (a) selective C5′,H5′-HSQC, (b) selective HCC5′H5′-COSY, and (c) selective HCC5′H5′-TOCSY used for the determination of ^2J(C4′,H5′) coupling constants in this study. The details of the parameters used to implement these pulse sequences are given in part B of the Experimental Section.

B. Measurement of ^2J(C4′,H5′) Coupling Constants. The family of C5′,H5′-selective experiments (the selective C5′,H5′-HSQC (heteronuclear single quantum spectroscopy), the selective HCC5′H5′-COSY, and the selective HCC5′H5′-TOCSY) designed to measure ^2J(C4′,H5′) coupling constants are shown in Figure 4. The core element found in all these experiment is the selective correlation of the C5′ carbon with the H5′ protons, while leaving the spin state of the C4′ carbon unperturbed. This is achieved in similar fashion in each of the experiments by using a selective C5′ carbon 90° pulse for the C5′ → H5′ back-transfer and selective carbon decoupling in ω_2.[24] This selective pulse sequence element was used previously to measure $^2J(H_\alpha,C')$ coupling constants in proteins.[25] In all experiments, E.COSY type[20,26] cross peaks (Figure 5b) are generated by allowing the relatively large associated ^1J(C4′,C5′) coupling to evolve during the C5′ chemical shift evolution which resolves the small ^2J(C4′,H5′) coupling that evolves during proton acquisition.

In the selective C5′,H5′-HSQC (Figure 4a), approximately 60% of the potential C5′,H5′ cross peaks were resolved so that their ^2J(C4′,H5′) coupling constants could be extracted. For this reason the 3D selective HCC5′H5′-COSY (Figure 4b) and 3D selective HCC5′H5′-TOCSY (Figure 4c) were implemented to resolve the C5′, H5′ cross peaks by labeling them in the ω_1 dimension with the chemical shift of either the C4′ carbon or the H1′ proton, respectively. The 3D selective HCC5′H5′-

(24) Eggenberger, U.; Schmidt, P.; Sattler, M.; Glaser, S. J.; Griesinger, C. *J. Magn. Reson.* **1992**, *100*, 604−610.
(25) Vuister, G.; Bax, A. *J. Biomol. NMR* **1992**, *2*, 401−405.
(26) Griesinger, C.; Sørensen, O. W.; Ernst, R. R. *J. Am. Chem. Soc.* **1985**, *107*, 6394−6396; Griesinger, C.; Sørensen, O. W.; Ernst, R. R. *J. Magn. Reson.* **1987**, *75*, 474−492.

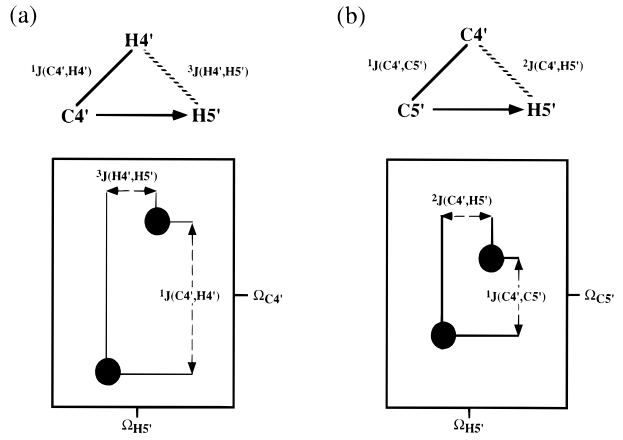

Figure 5. Schematic E.COSY multiplet pattern observed in the (a) HCC-TOCSY-CCH-E.COSY experiment and (b) C5′, H5′ selective experiments.

COSY experiment (Figure 4b) was designed to resolve cross peaks that belong to residues in nonhelical regions of the RNA structure. In these regions, such as the loop in this hairpin, the C4′ carbons are usually dispersed well enough to resolve the C5′, H5′ cross peaks. In the 3D selective HCC5′H5′-COSY experiment, the labeling of the C5′,H5′ cross peaks with the C4′ carbon resonances is obtained by a constant time carbon evolution of $3[4^1J(C,C)]^{-1}$ prior to the ^{13}C COSY pulse, which also serves simultaneously to generate antiphase carbon magnetization of the form $2C_{4y}C_{5z}$. The proton 90° pulse applied simultaneously with the second 90° ^{13}C pulse converts operators associated with non-refocused proton magnetization into nonobservable multiquantum coherence.

For the residues in the helical portion of the RNA where the C4′ carbons are severely overlapped, the 3D selective HCC5′H5′-TOCSY experiment (Figure 4c) was used to correlate the C5′,H5′ cross peaks to the usually well resolved H1′ protons. In this experiment, a C,C-TOCSY mixing period of 24 ms was chosen to obtain the maximum transfer from the C1′ to the C5′ carbon. The optimal C,C-TOCSY mixing period was extracted from transfer functions that were originally calculated for the aliphatic carbon spin systems found in amino acid side chains.[27] For the ribose five-carbon spin system with ^1J(C,C) ~40 Hz, the transfer function calculated for the five-carbon linear spin system of lysine was used with a simple rescaling of the ^1J(C,C) couplings from 35 to 40 Hz. The correlation to the H1′ proton via the C,C-TOCSY is the most favorable way to resolve most of the C5′,H5′ cross peaks, but it suffers in sensitivity with respect to the COSY experiment due the fact that magnetization that originates from the C1′ carbon is transferred to a certain extent over all carbons in the ribose ring. The choice of experiment should therefore be made on the basis of the requirements for resolution vs sensitivity in a given sample.

Both the HCC-TOCSY-CCH-E.COSY- and C5′H5′-selective experimental methods are relatively insensitive to strong coupling effects. It can be shown by simulations that strong coupling between the H5′ protons starts to systematically alter the size of the coupling constants extracted only when $\Delta\Omega < 2\pi\cdot 20$ Hz (data not shown). Nonetheless, even in the limit of strong coupling between H5′ protons, the sign of the ^2J(C4′,H5′) couplings remain true.

Results and Discussion

A. NMR Experiments. In the study of macromolecules (10−25 kDa), the precise determination of coupling constants from the multiplet patterns of simple COSY-type experiments is difficult due to the fact that line widths normally are of the same size or exceed the size of the couplings of interest. Moreover, in RNA molecules, severe chemical shift overlap of H2′, H3′, H4′, and H5′ ribose protons makes even an estimation of coupling constants from H,H-COSY cross peaks all but impossible. In macromolecules where the line widths are on the order of the coupling of interest, a partial cancellation of the antiphase components results in the observation of antiphase splittings that are systematically larger than the true coupling constant. By using the E.COSY method[20,26] only connected transitions are observed in a particular multiplet and therefore passive couplings can be measured without interference from components of opposite phase. Heteronuclear-based E.COSY methods, as discussed in this paper, utilize relatively large associated ^1J couplings to resolve the smaller couplings of interest and so allow the sign and magnitude of a coupling constant to be determined in macromolecules where the couplings are usually smaller than the line widths. As previously discussed,[28] however, the faster relaxation of the antiphase terms as compared to in-phase terms results in an observed value J^{eff} from an E.COSY-type multiplet which tends to be smaller than the actual coupling constant. For the measured ^3J(H4′,H5′) coupling constants, the effect of this differential relaxation leads to systematic errors when the correlation time, τ_c, becomes exceedingly large. In this case these coupling constants should be determined using the DQ/ZQ methodology[29] which largely suppresses differential relaxation effects. In contrast, the measured ^2J(C4′,H5′) couplings constants will only be affected by differential relaxation for correlation times, τ_c, that are greater than 100 ns because $^{13}C-^1H$ dipolar relaxation becomes less effective with increasing τ_c and $^{13}C-^{13}C$ dipolar relaxation can be neglected for $\tau_c < 100$ ns.

The schematic cross peaks of the correlated spins in a multiplet from the "directed" HCC-TOCSY-CCH-E.COSY experiment is shown in Figure 5a. As in the parent HCCH-E.COSY experiment,[21,22] a relatively large ^1J(C4′,H4′) heteronuclear coupling is used to displace the two components of the E.COSY cross peak multiplet in the inverse carbon dimension. The sign and magnitude of the passive ^3J(H4′,H5′) couplings is extracted from the displacement of two components of the E.COSY multiplet observed in the proton acquisition dimension. The schematic cross peak pattern for the family of selective C5′,H5′ experiments is shown in Figure 5b. In these experiments, the relatively large ^1J(C4′,C5′) homonuclear coupling is again utilized to displace the two components of the E.COSY multiplet in the inverse carbon dimension. As in the "directed" HCC-TOCSY-CCH-E.COSY experiment, the sign and magnitude of the passive ^2J(C4′,H5′) couplings is extracted from the displacement of two components of the E.COSY multiplet observed in the proton acquisition dimension.

B. Conformation Analysis of γ and Stereospecific Assignment of H5′$^{(pro\text{-}S)}$ and H5′$^{(pro\text{-}R)}$. The assignment of conformation about the angle γ to one of three possible staggered conformations (gauche$^+$, gauche$^-$, and trans) can be made using the ^3J(H4′,H5′) and ^2J(C4′,H5′) coupling constant signatures that are found for each of the three rotamers (Figure 1b). Each of the three rotamers (gauche$^+$, gauche$^-$, and trans) about γ shows a characteristic and distinguishable pattern of ^2J and ^3J coupling constants. In the canonical A-form geometry ($\gamma = 60°$, gauche$^+$), both ^3J(H4′,H5′) coupling constants are

(27) Eaton, H. L.; Fesik, S. W.; Glaser, S. J.; Drobny, G. P. *J. Magn. Reson.* **1990**, *90*, 452−463.

(28) Harbison, G. S. *J. Am. Chem. Soc.* **1993** *115*, 3026. Norwood, T. J. *J. Magn. Reson. A* **1993**, *104*, 106. Norwood, T. J. *J. Magn. Reson. A* **1993**, *101*, 109.

(29) Rexroth, A.; Schmidt, P.; Szalma, S.; Geppert, T.; Schwalbe, H.; Griesinger, C. *J. Am. Chem. Soc.* **1995**, *117*, 10389−10390.

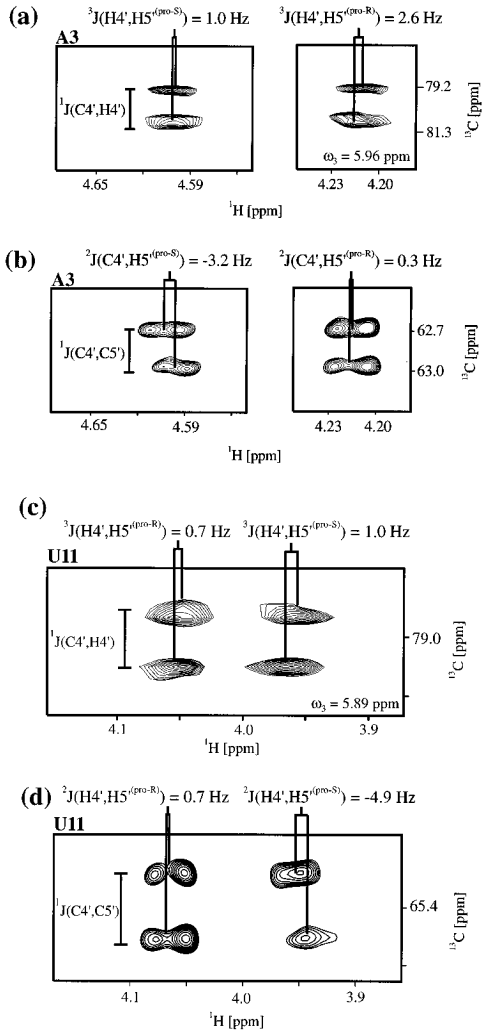

Figure 6. Expansion of the regions from the 3D "directed" HCC-TOCSY-CCH-E.COSY showing the C4′,H5′ cross peaks associated with (a) residue A3 (H1′ plane of A3, $\omega_1 = 5.96$ ppm) and (c) residue U11 (H1′ plane of U11, $\omega_1 = 5.89$ ppm) and an expansion of the 2D C5′,H5′ selective HSQC experiments showing the C5′,H5′ cross peaks observed for (b) residue A3 and (d) residue U11 of the 19-mer RNA hairpin.

expected to be small and positive. For this rotamer conformation, the ^2J(C4′,H5′$^{(pro-S)}$) coupling constant is expected to be large and negative and the ^2J(C4′,H5′$^{(pro-R)}$) coupling constant is expected to be small and positive, which yields the stereospecific assignment of the H5′ protons. In the other rotamer states (i.e. trans and gauche$^-$), one large and one small ^3J(H4′,H5′) coupling constant is expected. To distinguish the trans and gauche$^-$ conformers, stereospecific assignment of the H5′$^{(pro-S)}$ and H5′$^{(pro-R)}$ protons using the signs of the ^2J(C4′,H5′$^{(pro-S)}$) and ^2J(C4′,H5′$^{(pro-R)}$) coupling constants is necessary.

The E.COSY cross peak patterns observed in the "directed" HCC-TOCSY-CCH-E.COSY and the selective C5′,H5′-HSQC for residues A3 and U11 are shown in Figure 6. The E.COSY cross peak patterns shown for residues A3 and U11 are representative of those observed for stem and loop residues, respectively. For the A3 residue, the ^3J(H4′,H5′) coupling constants measured in the "directed" HCC-TOCSY-CCH-E.COSY experiment (Figure 6a) were found to be both small (1.0 and 2.6 Hz) and positive. In the selective C5′,H5′ HSQC experiment (Figure 6b), the coupling constant measured for the downfield C5′, H5′ cross peak was found to be relatively large (−3.2 Hz) and negative, while the coupling constant measured for the upfield C5′, H5′ cross peak was found to be small (0.3 Hz) and positive. This leads to the stereospecific assignment of the downfield proton to H5′$^{(pro-S)}$ and the upfield proton to H5′$^{(pro-R)}$. For the U11 residue, the ^3J(H4′,H5′) coupling constants measured in the "directed" HCC-TOCSY-CCH-E.COSY experiment (Figure 6c) were also both found to be small (0.7 and 1.0 Hz) and positive. In the selective C5′,H5′ HSQC experiment (Figure 6d), the coupling constant measured for the downfield C5′, H5′ cross peak was found to be small (0.7 Hz) and positive, while the coupling constant measured for the upfield C5′, H5′ cross peak was found to be relatively large (−4.9 Hz) and negative. In contrast to residue A3, this pattern leads to the stereospecific assignment of the downfield proton to H5′$^{(pro-R)}$ and the upfield proton to H5′$^{(pro-S)}$. In Table 1 it can be seen that all the measured ^3J(H4′,H5′) coupling constants were found to be relatively small (∼1−5 Hz) and that no significant distinction in the coupling patterns was observed between the stem and loop residues of this hairpin. This indicates that all residues (independent of the secondary structure element) in the hairpin have γ angles that are in a gauche$^+$ conformation (Figure 1b). The rather uniform gauche$^+$ conformation observed for all γ angles in this hairpin seems to suggest that γ is not involved in any loop "kinks" or turns.

The signs and magnitudes of the ^2J(C4′,H5′) coupling constants that were used to stereospecifically assign the H5′ protons as either pro-S or pro-R for the residues in the 19-mer RNA hairpin are also shown in Table 1, with the observed chemical shifts for the more downfield H5′ protons highlighted in bold. For the residues in the helical stem region of the hairpin, with the exception of residue G13, all the more downfield resonating H5′ protons have been assigned to H5′$^{(pro-S)}$. This is in agreement with the expected chemical shift for a nucleotide in a helical conformation[3,10] and follows the original chemical shift rules proposed by Remin and Shugar.[5] Within the loop region (residues U8 through A12) of the hairpin, with the exception of residue U8, the H5′$^{(pro-R)}$ protons were found to resonate slightly downfield of the H5′$^{(pro-S)}$ proton. The correlation of stereospecific assignment and chemical shift for these H5′ protons was therefore opposite from what was observed for the residues in the helical stem region. In addition, the proton chemical shift differences between the H5′$^{(pro-S)}$ and H5′$^{(pro-R)}$ resonances were found to be smaller and less regular than for the H5′$^{(pro-S)}$ and H5′$^{(pro-R)}$ resonances found in the helical stem, where the chemical shift differences between the H5′ resonances were found usually to be ∼0.4 ppm. For the loop residues, the proton chemical shift differences observed between the H5′ protons in the loop were found to be less than 0.1 ppm (Table 1).

An inversion of the chemical shifts of the H5′$^{(pro-S)}$ and H5′$^{(pro-R)}$ resonances similar to the one described here for the RNA I hairpin has been observed in UUCG tetraloop RNA, where the stereospecific assignment of the H5′ protons has been determined.[10] From the measured signs of the ^2J(C4′,H5′) coupling constants about γ in the UUCG tetraloop,[10] the more downfield proton was assigned to H5′$^{(pro-R)}$, rather than H5′$^{(pro-S)}$ for residues C7 and G8, which are both found within the U6−G8 loop of the hairpin. In a DNA TTTA tetraloop hairpin studied by Blommers and co-workers,[6] the more downfield proton was assigned to H5′$^{(pro-R)}$, rather than H5′$^{(pro-S)}$ for residues T3 and A4, which are also both found within the T1−A4 loop of this hairpin.

A plot of the C5′, H5′ region of a normal constant time ^{1}H,^{13}C-HSQC is shown in Figure 7a with cross peaks labeled according to their stereospecific assignment (bold cross peaks indicate an assignment of the H5′ proton resonance to pro-S

Table 1. C5′ and H5′ Chemical Shifts and ^3J(H4′,H5′) and ^2J(C4′,H5′) Couplings about γ Determined for the 19-mer RNA

residue	Ω(C5′)[a]	Ω(H5′$^{(S)}$)[a]	^3J(H4′,H5′$^{(S)}$)[b]	^2J(C4′,H5′$^{(S)}$)[b]	Ω(H5′$^{(R)}$)[a]	^3J(H4′,H5′$^{(R)}$)[b]	^2J(C4′,H5′$^{(R)}$)[b]
1	64.19	**4.34**[d]	nd[c]	nd[c]	4.23[d]	nd[c]	nd[c]
2	65.06	**4.10**	2.6	−3.4	4.00	nd[c]	−0.5
3	62.82	**4.60**	1.0	−3.2	4.21	2.6	0.3
4	62.41	**4.51**	1.0	−3.7	4.06	<0.2	0.8
5	62.86	**4.48**	<1.0	−3.9	4.00	1.4	0.6
6	62.44	**4.47**	1.0	−5.1	4.06	<1.0	−0.2
7	62.10	**4.45**[d]	2.1	nd[c]	4.03[d]	<1.0	nd[c]
8	63.99	**4.27**	1.0	−4.9	4.02	1.1	1.4
9	65.38	4.00	3.0	−5.1	**4.05**	4.4	1.0
10	65.36	4.02	2.5	−5.4	**4.06**	2.3	1.2
11	65.66	3.93	1.0	−4.9	**4.02**	0.7	0.7
12	65.98	4.30	<1.0	−3.0	**4.32**	<1.0	<1.0
13	65.55	4.28	0.7	−4.3	**4.37**	<1.0	0.2
14	62.33	**4.46**	<0.2	−6.7	4.05	1.0	−1.5
15	63.61	**4.45**	2.7	−4.3	4.11	<1.0	−1.4
16	63.23	**4.47**	1.3	−5.0	4.06	1.6	−1.2
17	62.19	**4.54**[d]	<1.0	nd[c]	4.03[d]	<1.0	nd[c]
18	62.95	**4.54**	0.6	−3.0	4.10	0.6	−1.0
19	65.22	**4.01**[d]	nd[c]	nd[c]	3.94[d]	nd[c]	nd[c]

[a] The chemical shift of the proton and carbon resonances is given in parts per million. [b] The ^3J and ^2J coupling constants are given in hertz. [c] nd. = stereospecific assignment not determined due to chemical shift overlap of the residue cross peaks. [d] For H5′ protons that have not been stereospecifically assigned, the more downfield resonance is listed in the H5′$^{(pro\text{-}S)}$ column. The proton chemical shifts of the more downfield H5′ resonances are highlighted in bold.

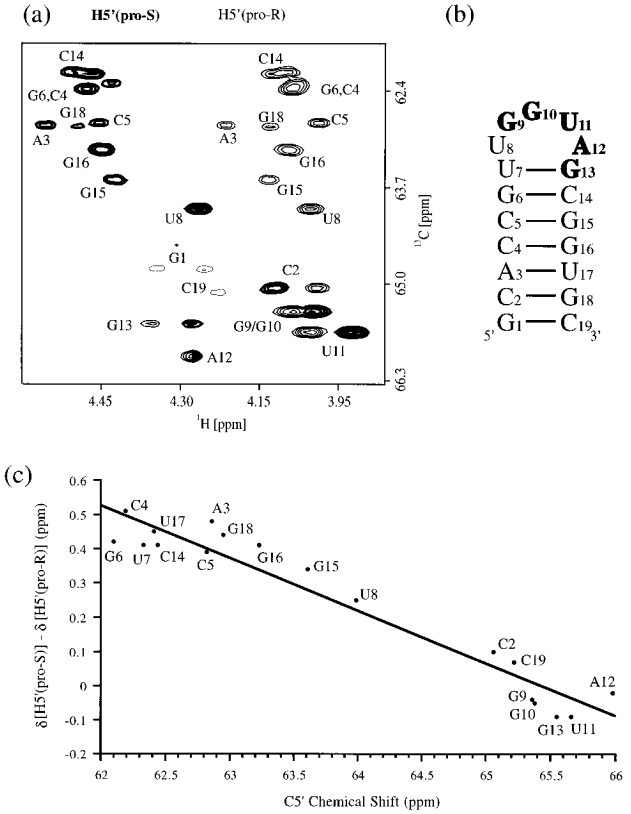

Figure 7. (a) Expanded plot of the C5′, H5′ region of a constant time HSQC performed on the 19-mer RNA hairpin with the residue cross peak assignments indicated. The cross peaks stereospecifically assigned to H5′$^{(pro\text{-}S)}$ and H5′$^{(pro\text{-}R)}$ protons are shown with bold and normal lines, respectively. (b) Schematic of the secondary structure of the 19-mer RNA hairpin with residues having "noncanonical" proton chemical shifts for their H5′$^{(pro\text{-}S)}$ and H5′$^{(pro\text{-}R)}$ protons highlighted in bold. (c) Plot of the C5′ carbon versus the difference in H5′$^{(pro\text{-}S)}$ and H5′$^{(pro\text{-}R)}$ proton chemical shifts (ppm) for each of the stereospecifically assigned residues in the 19-mer hairpin together with a best-fit line (the correlation coefficient R is −0.96) to show the general anticorrelation trend observed for the chemical shifts of these resonances.

and thin-lined cross peaks indicates an assignment of the H5′ proton resonance to pro-R). Figure 7b shows a schematic of the secondary structure of the RNA I hairpin and indicates the position in bold of the residues for which the more downfield proton is assigned to H5′$^{(pro\text{-}R)}$, rather than H5′$^{(pro\text{-}S)}$ as normally predicted in a double-helical conformation. It is interesting to note that there is an overall anticorrelation of the C5′ carbon chemical shifts and the difference of the H5′ proton chemical shifts for the residues of this hairpin (Figure 7c).

Currently, the available data base of oligonucleotides for which the stereospecific assignment of H5′ protons has been determined and from which the chemical shift patterns of the H5′$^{(pro\text{-}S)}$ and H5′$^{(pro\text{-}R)}$ protons can be predicted is quite limited. In the 19-mer RNA hairpin investigated here, the phenomenological observation that the chemical shift patterns correlate with the secondary structure shifted by one residue toward the 3′ end of the primary sequence (Figure 7b) hints at an influence of the preceding nucleotide on the chemical shifts of the H5′ protons of each particular nucleotide. Although intranucleotide influences on the differential shielding of the H5′ protons can not be ignored, it is interesting to note that *ab initio* quantum mechanical calculations on 3′- and 5′-phosphate mononucleotide systems[30] predict that the chemical shielding for the H5′ protons should be rather equivalent in both C2′-endo and C3′-endo sugar conformations when the backbone angles β, γ, and ϵ assume canonical conformations.

A possible means via which the preceding nucleotide could influence the chemical shifts of the H5′ protons is through hydrogen bonding networks involving the preceding ribose 2′ OH. In A-form RNA where the ribose sugars are in a C3′-endo conformation, a hydrogen bridge can potentially form between the 2′ OH$_{(i-1)}$ hydroxyl and O4′$_{(i)}$ and a water-mediated hydrogen bridge can potentially form between the 2′ OH$_{(i-1)}$ hydroxyl and PO$_{(i)}$. Both interactions, although probably weak and transient, are unique to the A-form geometry and are not seen for C2′-endo sugar puckers.[31] Since a significant C2′-endo conformation is found for all the loop residues (U8 through A12),[16] the inverted pattern of H5′ chemical shifts observed for residues G9 through G13 corroborates this interpretation. This mechanism of influence on the chemical shifts also provides a potential explanation for the observed anticorrelation between the chemical shifts of the C5′ carbon resonances and

(30) Giessner-Prettre, C.; Pullman, B. *Q. Rev. Biophys.* **1987**, *20*, 113−172.

(31) Sänger, W. *Principles of Nucleic Acid Structure*; Springer-Verlag: New York, 1988.

difference in the chemical shifts of H5′ proton resonances since it is well-known that perturbations in the electronic network of a molecule can have an alternating through-bond effect on the chemical shifts of atoms that are distant from the perturbation by differing numbers of intervening bonds.[32] A similar "shifted" pattern of correlation between H5′ chemical shifts and the secondary structure is also observed in the UUCG tetraloop, where a significant C2′-endo conformation is found for the loop residues (U6 and C7) and an inverted pattern of H5′ chemical shifts is observed for residues C7 and G8.

We propose this model for the interpretation of the H5′ chemical shifts with some confidence because the only gross conformational change observed in the backbone geometry of this RNA hairpin seems to be confined to the backbone angle δ. In contrast, the backbone angles β, γ, and ϵ all appear not to vary significantly from the expected canonical A-form geometry as determined from measuring ^3J(H,P) and ^3J(H,H) coupling constants (data not shown). In addition, although the angles α and ζ cannot be measured directly, none of the observed phosphorus chemical shifts are significant outliers, indicating a rather uniform behavior for α and ζ.[33] In addition, we also have an indication in the RNA loop that the angle χ does not play a decisive role in determining the chemical shift of the H5′ protons since residues G9 and G10, which are both found to be in the syn conformation,[33] are not significant outliers from the observed chemical shift patterns.

Conclusion

In summary, we present here robust methods for the measurement of ^3J(H4′,H5′) and ^2J(C4′,H5′) coupling constants in uniformly ^{13}C labeled oligonucleotides. These NMR methods have been demonstrated to unambiguously determine the backbone angle γ and stereospecifically assign H5′ protons in a uniformly ^{13}C labeled RNA hairpin. They rely on through-bond heteronuclear correlation of resonances and therefore in contrast to NOE-based methods do not have the drawback of poor resolution and low sensitivity. Like in NOE-based methods, however, conformational averaging will also make it difficult to unambiguously interpret a measured coupling constant. The NMR methods proposed here can be easily extended to the stereospecific assignment of H5′ protons in uniformly ^{13}C labeled DNA. In addition, the selective C5′,H5′ correlation methods presented here can be adapted to measure other ^2J(C,H) couplings in uniformly ^{13}C labeled oligonucleotides and thereby provide further information about sugar pucker conformations and dynamics.

Experimental Section

A. Sample Preparation. The 19-mer RNA stem-loop, derived from the RNA I transcript of the *Col E1* replication control system,[34] was synthesized by T7 run-off transcription and purified using standard gel electrophoresis methods. The ^{13}C,^{15}N labeled NTPs were prepared from RNA isolated from *Methylophylus Methylotrophs* grown in minimal media with [^{13}C]methanol and $^{15}NH_4Cl$ as the sole carbon and nitrogen sources, respectively. The monomeric state of the 19-mer RNA stem−loop at the NMR concentrations (∼1.5 mM) used in this study has been documented by mobility shift gel electrophoretic analysis.[33] The NMR sample was prepared to contain ∼1.5 mM oligonucleotide in 99.9996% D_2O, 25 mM NaCl, 1 mM $MgCl_2$, and 1 mM cacodylate [pH = 6.5]. The experiments were measured in a Shigemi limited-volume NMR tube with a sample volume of ∼180 μL. The complete resonance assignment of the 19-mer RNA I stem-loop, with the exception of stereospecific assignment of H5′ protons, has previously been determined.[33]

B. Acquisition and Processing of NMR Data. The "directed" HCC-TOCSY-CCH-E.COSY experiment, the C5′,H5′-selective HSQC experiment, the selective HCC5′,H5′-COSY experiment, and the selective HCC5′H5′-TOCSY experiment were all recorded at 298 K on a Bruker AMX-600 spectrometer equipped with a triple-resonance broad-band probe with actively shielded gradients and linear amplifiers on all three channels. All spectra were processed using Felix 2.30 software (Biosym Technologies) on a Silicon Graphics workstation.

The "directed" HCC-TOCSY-CCH-E.COSY experiment used in this study is shown schematically in Figure 2. Narrow and wide pulses denote 90° and 180° flip angle pulses, respectively. The proton β = 45° pulse was implemented as a pair of 90° pulses that were phase shifted by β. The eight-step phase cycle was as follows: $\phi_1 = 2(x), 2(-x)$, $\phi_2 = x,-x$; $\phi_3 = 4(x),4(-x)$, rec = $(x,-x,-x,x)$. The delays were Δ = 3 ms, $\sim[2^1J(C,H)]^{-1}$; Δ' = 3.0 ms, $\sim[2^1J(C,H)]^{-1}$, which is optimized for the transfer of the CH groups and τ = 6.25 ms, $\sim[4^1J(C,C)]^{-1}$. The C,C-TOCSY was accomplished using DIPSI-3,[35] with $\gamma B_1/2\pi$ = 6.0 kHz and a mixing time of 13.5 ms, and the constant time period T = 7.6 ms. The carbon transmitter frequency was centered on the ribose region of the spectrum (∼80 ppm), and the proton transmitter was centered on the residual HDO signal (4.75 ppm). ^{13}C decoupling was achieved with GARP[36] using $\gamma B_1/2\pi$ = 2.0 kHz. ^{31}P decoupling was achieved with GARP using $\gamma B_1/2\pi$ = 1.25 kHz. Quadrature detection was obtained in ω_1 by incrementing ϕ_1 and in ω_2 by incrementing all carbon pulses after the t_2 evolution according to States-TPPI.[37]

The HCC-TOCSY-CCH-E.COSY experiment was collected with 512 (t_3^{max} = 128 ms), 36 (t_2^{max} =7.6 ms), and 46 (t_1^{max} = 24 ms) complex points in ω_3, ω_2, and ω_1, respectively. Sixteen scans per t_1, t_2 increment were collected with spectral widths of 4000, 5000, and 2000 Hz in ω_3, ω_2, and ω_1, respectively. Total experiment time was 48 h. Mirror image linear prediction[38] was used to expand ω_2 from 36 to 118 complex points using 24 poles and 12 peaks. Square cosine bell apodization and zero-filling was applied in all dimensions, with strip transformation from 6.1 to 3.8 ppm in ω_3 yielding a final matrix size of 512 × 128 × 128 real points in ω_3, ω_2, and ω_1, respectively.

The family of selective C5′,H5′ experiments used in this study is shown schematically in Figure 4. Narrow and wide pulses denote 90° and 180° flip angle pulses, respectively. Gaussian selective 90° pulses are drawn schematically. Selective C5′ decoupling was achieved using MLEV-16 expansions of G3-pulses.[21] ^{31}P decoupling was achieved using a WALTZ sequence ($\gamma B_1/2\pi$ = 1.25 kHz). Selective inversion G3-pulses[40] used for the decoupling of C5′ carbons during acquisition were applied with a duration of 4.096 ms, and the selective 90° G4 and time-reversed G4-pulses[39] were applied with durations of 3.2 ms. All selective pulses used a 5% truncation factor.

The selective C5′,H5′-HSQC (Figure 4a) employed an eight-step phase as follows: $\phi_1 = 4(x), 4(-x)$, $\phi_2 = x,-x$; $\phi_3 = 2(x),2(-x)$, rec = $(x,-x,-x,x)$, $(-x,x,x,-x)$. The delay Δ = 3.0 ms, $\sim^1/_2$J(C,H). The two carbon 90° pulses were applied as Gaussian G4- and time-reversed G4-pulses for the selective excitation of the C5′ resonances. The carbon transmitter frequency was centered in the middle of the C5′ carbons (∼63.5 ppm), and the proton transmitter was centered on the residual HDO signal (4.75 ppm). Quadrature detection was obtained in the ω_1 dimension by cycling phase ϕ_2 according to States-TPPI.[37] The selective C5′H5′-HSQC experiments with 16 scans per t_1 increment were collected with 190 (t_1^{max} = 23.75 ms) and 2048 (t_2^{max} = 512 ms) complex points recorded in ω_1 and ω_2, respectively. Total experiment time was 2.5 h. Lorentz-to-Gauss transformation was used to enhance the resolution in the H5′, C5′ cross peak region and by comparing the extracted couplings of well-resolved cross peaks at different levels of resolution enhancement; an internal check was available to ensure that

(32) Buckingham, A. D. *Can. J. Chem.* **1961**, *38*, 300.
(33) Marino, J. P. Thesis, Yale University, 1995.
(34) Eguchi, Y.; Itoh, T.; Tomizawa, J. *Annu. Rev. Biochem.* **1991**, *60*, 631−652. Eguchi, Y.; Tomizawa, J. *J. Mol. Biol.* **1991**, *220*, 831−842.
(35) Shaka, A. J.; Lee, C. J.; Pines, A. *J. Magn. Reson.* **1988**, *77*, 274−293.
(36) Shaka, A. J.; Barker, P.; Freeman, R. J. *J. Magn. Reson.* **1985**, *64*, 547−552.
(37) Marion, D.; Ikura, R.; Tschudin, R.; Bax, A. *J. Magn. Reson.* **1989**, *85*, 393.
(38) Zhu, G.; Bax, A. *J. Magn. Reson.* **1990**, *90*, 405−410.
(39) Emsley, L.; Bodenhausen, G. *J. Magn. Reson.* **1989**, *82*, 211−221. Emsley, L.; Bodenhausen, G. *Chem. Phys. Lett.* **1990**, *165*, 469−476.

no artifacts had been introduced by the apodization. The data were zero-filled and strip-transformed from 4.75 to 3.8 ppm in ω_2 to yield a final matrix size of 1024 × 1024 real points.

The selective HCC5′H5′-COSY (Figure 4b) employed a four-step phase as follows: $\phi_1 = 2(x), 2(-x)$, $\phi_2 = x,-x$; rec = $(x,-x,-x,x)$. The delays were Δ = 3.0 ms, $\sim[2^1J(C,H)]^{-1}$; Δ' = 2.2 ms, $\sim[4^1J(C5',H5')]^{-1}$; and T = 18.75 ms, $\sim 3[4^1J(C,C)]^{-1}$. The final carbon 90° pulse was applied as a G4-pulse for the selective excitation of the C5′ resonances. The carbon transmitter frequency was centered in the middle of the C5′ carbons (∼63.5 ppm), and the proton transmitter was centered on the residual HDO signal (4.75 ppm). Quadrature detection was obtained in ω_1 by cycling ϕ_1 and in ω_2 by cycling all carbon pulses after the t_2 evolution according to States-TPPI.[37] The selective HCC5′H5′-COSY experiment was collected with 58 (t_1^{max} = 14.5 ms), 36 (t_2^{max} = 48.3 ms), and 512 (t_3^{max} = 128 ms) complex points recorded in ω_1, ω_2, and ω_3, respectively. Eight scans per t_1, t_2 increment were collected with spectral widths of 4000, 1200, and 4000 Hz in ω_3, ω_2, and ω_1, respectively. Total experiment time was 28 h. A linear phase correction[40] was applied in the t_1 dimension to shift the center of the carbon spectrum downfield by ∼2500 Hz from 63.5 ppm (C5′ center) to 80 ppm (center of the ribose carbons). Mirror image linear prediction[38] was used to expand ω_1 from 58 to 174 complex points using 24 poles and 12 peaks, and linear prediction was used to expand ω_2 from 36 to 72 complex points using 12 poles and 6 peaks. Square sine bell apodization shifted by 60° was applied in all dimensions, and the data were zero-filled, with strip transformation from 4.75 to 3.8 ppm in ω_3 to yield a final matrix size of 512 × 128 × 256 real points in ω_3, ω_2, and ω_1, respectively.

The selective HCC5′H5′-TOCSY (Figure 4c) employed a four-step phase as follows: $\phi_1 = x$; $\phi_1 = 2(x), 2(-x)$; $\phi_2 = x,-x$; rec = $(x,-x,-x,x)$. The delays were Δ = 3.0 ms, $\sim[2^1J(C,H)]^{-1}$; Δ' = 2.2 ms, $\sim[4^1J(C5',H5')]^{-1}$. The C,C-TOCSY was accomplished using DISPI-2,[35] with $\gamma B_1/2\pi$ = 6 kHz and a mixing time of 24 ms. The carbon transmitter frequency was centered in the middle of the ribose carbons (∼80 ppm), and the proton transmitter was centered on the residual HDO signal (4.75 ppm). The final carbon 90° pulse was applied as an off-resonance Gaussian G4-pulse (centered at ∼63.5 ppm) for the selective excitation of the C5′ resonances. Quadrature detection was obtained in ω_1 by cycling ϕ_1 and in ω_2 by cycling all carbon pulses after the t_2 evolution according to States-TPPI.[37] The selective HCC5′H5′-TOCSY experiment was collected with 92 (t_1^{max} = 36.8 ms), 32 (t_2^{max} = 40 ms), and 512 (t_3^{max} = 128 ms) complex points recorded in ω_1 and ω_2, respectively. Eight scans per t_1, t_2 increment were collected with spectral widths of 4000, 800, and 2500 Hz in ω_3, ω_2, and ω_1, respectively. Total experiment time was 40 h. Linear prediction was used to expand ω_1 from 92 to 184 complex points using 32 poles and 16 peaks. Square sine bell apodization shifted by 60° was applied in all dimensions, and the data were zero-filled, with strip transformation from 4.75 to 3.8 pm in ω_3 to yield a final matrix size of 128 × 64 × 256 real points in ω_3, ω_2, and ω_1, respectively.

C. Coupling Constant Determination. The $^3J(H4',H5')$ and $^2J(C4',H5')$ coupling constants were determined by first extracting the appropriate rows in ω_3 of a "directed" HCC-TOCSY-CCH-E.COSY, ω_2 of a selective C5′,H5′-HSQC, and ω_3 of the selective HCC5′H5′-COSY and selective HCC5′H5′-TOCSY. For each E.COSY multiplet, two ω_3 traces corresponding to the upfield and downfield components of the multiplet were obtained by a summation of the slices that comprise each of the multiplet components. The coupling constants were fit using a procedure of minimizing the power difference spectrum in the time domain after subtraction of the two respective rows extracted from the cross peaks of the observed E.COSY multiplet. The details of the fitting procedure and error analysis have been previously described.[41]

Acknowledgment. This work was supported by the Fonds der Chemischen Industrie and the DFG under Gr1211/2-3. J.P.M acknowledges support by Prof. Crothers through NIH Grant GM 21966 and by an Alexander von Humboldt Post-Doctoral Fellowship. H.S. was supported by a stipend of the EU (Human Capital and Mobility). S.J.G. is supported by the DFG through a Heisenberg Stipendium Gl 203/2-1. H.S. thanks Chris Dobson for encouragement. We thank one of the reviewers who pointed out that the anticorrelation between the difference in H5′ proton chemical shifts and the C5′ carbon chemical shift was stronger than that between the $H5'^{(pro\text{-}S)}$ chemical shift and the C5′ carbon chemical shift.

JA953554O

(40) Bax, A.; Ikura, M.; Kay, L. E.; Zhu, G. *J. Magn. Reson.* **1991**, *91*,174−178.

(41) Schwalbe, H.; Samstag, W.; Engels, J. W.; Bermel, W.; Griesinger, C. *J. Biomol. NMR* **1993**, *3*, 479−486.